INFLAMMATION

MerTK signaling in macrophages promotes the synthesis of inflammation resolution mediators by suppressing CaMKII activity

Bishuang Cai[1]*, Canan Kasikara[1], Amanda C. Doran[1], Rajasekhar Ramakrishnan[2], Raymond B. Birge[3], Ira Tabas[1]*

Inflammation resolution counterbalances excessive inflammation and restores tissue homeostasis after injury. Failure of resolution contributes to the pathology of numerous chronic inflammatory diseases. Resolution is mediated by endogenous specialized proresolving mediators (SPMs), which are derived from long-chain fatty acids by lipoxygenase (LOX) enzymes. 5-LOX plays a critical role in the biosynthesis of two classes of SPMs: lipoxins and resolvins. Cytoplasmic localization of the nonphosphorylated form of 5-LOX is essential for SPM biosynthesis, whereas nuclear localization of phosphorylated 5-LOX promotes proinflammatory leukotriene production. We previously showed that MerTK, an efferocytosis receptor on macrophages, promotes SPM biosynthesis by increasing the abundance of nonphosphorylated, cytoplasmic 5-LOX. We now show that activation of MerTK in human macrophages led to ERK-mediated expression of the gene encoding sarcoplasmic/endoplasmic reticulum calcium ATPase 2 (SERCA2), which decreased the cytosolic Ca^{2+} concentration and suppressed the activity of calcium/calmodulin-dependent protein kinase II (CaMKII). This, in turn, reduced the activities of the mitogen-activated protein kinase (MAPK) p38 and the kinase MK2, resulting in the increased abundance of the nonphosphorylated, cytoplasmic form of 5-LOX and enhanced SPM biosynthesis. In a zymosan-induced peritonitis model, an inflammatory setting in which macrophage MerTK activation promotes resolution, inhibition of ERK activation delayed resolution, which was characterized by an increased number of neutrophils and decreased amounts of SPMs in tissue exudates. These findings contribute to our understanding of how MerTK signaling induces 5-LOX–derived SPM biosynthesis and suggest a therapeutic strategy to boost inflammation resolution in settings where defective resolution promotes disease progression.

INTRODUCTION

Timely resolution responses after acute inflammation are essential for tissue homeostasis (*1*, *2*), and impaired resolution is the underlying cause of various chronic inflammatory diseases, including cardiovascular disease, inflammatory bowel disease, multiple sclerosis, arthritis, and asthma (*3*–*7*). Inflammation resolution is an active, highly coordinated process that is controlled by various endogenous specialized proresolving mediators (SPMs), such as lipoxins, resolvins, protectins, and maresins (*1*, *8*, *9*). SPMs counterbalance proinflammatory mediators during acute inflammation and trigger resolution by blocking neutrophil infiltration, enhancing the clearance of dead cells (efferocytosis), and repairing tissue damage without compromising host defense (*1*, *10*).

SPMs are synthesized by lipoxygenase (LOX) enzymes from long-chain fatty acids, such as arachidonic acid (AA), which is released from phospholipids by the action of cytosolic phospholipase A_2; docosahexaenoic acid (DHA); and eicosapentaenoic acid (EPA) (*11*). We and others have shown that the intracellular localization of 5-LOX determines whether it stimulates the production of proinflammatory leukotrienes or proresolving lipoxins. Nuclear 5-LOX, because of its proximity to leukotriene A_4 (LTA_4) hydrolase, leads to the conversion of AA to leukotrienes (LTB_4) in macrophages (*12*–*14*). In contrast, cytoplasmic 5-LOX, because of its proximity to 12/15-LOX, which is the murine ortholog of human 15-LOX and has both 12-LOX and 15-LOX activities (*15*–*17*), promotes the conversion of AA to lipoxins (LXA_4) or DHA to resolvins (RvD1) (*14*). The nuclear localization of 5-LOX is mediated by its phosphorylation at Ser^{271} by mitogen-activated protein kinase (MAPK)–activated protein kinase 2 (MK2), which is downstream of the MAPK p38 (*13*, *18*). Previous work showed that a p38-MK2 pathway is activated by cytosolic Ca^{2+}-dependent calcium/calmodulin-dependent protein kinase II (CaMKII) (*14*, *19*, *20*), and we showed previously that Ca^{2+}-mediated CaMKII activation in macrophages increases the abundance of proinflammatory LTB_4 and decreases the amount of proresolving LXA_4 (*14*). However, the upstream regulators of CaMKII in this 5-LOX–derived SPM biosynthesis pathway remain unknown.

MerTK, a member of the Tyro-Axl-MerTK (TAM) family of receptor tyrosine kinases, is a macrophage receptor that mediates the binding and phagocytosis of apoptotic cells, a process known as efferocytosis. MerTK interacts with apoptotic cells through the bridging molecules Gas6 or protein S, which bind to MerTK on macrophages and to externalized phosphatidylserine on apoptotic cells (*21*, *22*). In addition to mediating efferocytosis, engagement of MerTK by apoptotic cells, Gas6, or protein S triggers two integrated but biochemically distinct responses: anti-inflammation and proresolution. Loss of these responses by genetic targeting of MerTK in mice can lead to chronic diseases of inflammation and impaired resolution, notably a lupus-like disease in older mice and atherosclerosis in hypercholesterolemic mice (*23*–*26*). The anti-inflammatory response involves a pathway that leads to the suppression of nuclear factor κB (NF-κB)–mediated signaling (*27*, *28*). Evidence for a distinct proresolution response was revealed by studies using both cultured macrophages and various in vivo models (*29*, *30*). For example, we demonstrated that MerTK signaling in macrophages and

[1]Departments of Medicine, Pathology and Cell Biology, and Physiology, Columbia University, New York, NY 10032, USA. [2]Department of Pediatrics, Columbia University, New York, NY 10032, USA. [3]Department of Microbiology, Biochemistry and Molecular Genetics, Rutgers University, New Jersey Medical School Cancer Center, Newark, NJ 07103, USA.
*Corresponding author. Email: bc2586@columbia.edu (B.C.); iat1@columbia.edu (I.T.)

in mouse models of sterile peritonitis and ischemia-reperfusion injury promotes SPM biosynthesis and enhances resolution by decreasing the amount of 5-LOX phosphorylated at Ser^{271} (p–Ser^{271}–5-LOX) and increasing the abundance of cytoplasmic 5-LOX (*30*). Moreover, the ectodomain of MerTK can be cleaved by the protease ADAM metallopeptidase domain 17 (ADAM17), and in mice harboring a genetically engineered form of MerTK that is cleavage-resistant ($Mertk^{CR}$), SPM biosynthesis and inflammation resolution are enhanced, and atherosclerosis progression is suppressed (*26*, *30*).

The objective of this study was to address a critical gap in this field, namely, the mechanism by which MerTK activation triggers resolution signaling in macrophages. More specifically, we sought to understand how engagement of MerTK increases the abundance of nonphosphorylated, cytoplasmic 5-LOX and the subsequent biosynthesis of LXA_4 and RvD1. We showed that the Gas6-MerTK pathway suppressed the aforementioned Ca^{2+}–CaMKII–p38–MK2–p–5-LOX signaling pathway by decreasing the concentration of cytosolic Ca^{2+}. Cytosolic Ca^{2+} abundance was decreased through MerTK-mediated activation of the MAPK extracellular signal–regulated kinase (ERK), which, in turn, stimulated the activity of SERCA, the calcium ATPase that pumps cytoplasmic Ca^{2+} back into the endoplasmic reticulum.

RESULTS

Gas6, through MerTK, suppresses the phosphorylation of CaMKII, p38, MK2, and 5-LOX and increases the ratio of lipoxins to leukotrienes in human monocyte–derived macrophages

RvD1 increases the abundance of nonphosphorylated, cytoplasmic 5-LOX and the production of LXA_4 in macrophages by suppressing the CaMKII–p38–MK2 cascade (*14*). Given that MerTK activation also affects 5-LOX and LXA_4 in a similar manner (*30*), we investigated the effect of MerTK activation on these three kinases. Human monocyte–derived macrophages (referred to as "human macrophages" throughout the study) were treated with *MERTK*-specific small interfering RNA (siRNA) or scrambled control siRNA and then incubated with conditioned medium from HEK 293 cells expressing the MerTK activator Gas6 or control conditioned medium. Cell extracts were then analyzed by immunoblot for the phosphorylated forms of the three kinases as a measure of their activation. Consistent with our previous findings from mouse macrophages (*30*), treatment of human macrophages with Gas6 increased the abundance of p-MerTK (Fig. 1A). As was the case with RvD1 in a previous study (*30*), Gas6 reduced the abundances of p-CaMKII, p-p38, and p-MK2 in scrambled siRNA–treated macrophages, and Gas6 reduced the abundance of p–Ser^{271}–5-LOX (Fig. 1A). The bands corresponding to the total and phosphorylated forms of MK2 and 5-LOX were at the correct molecular mass and were verified by the demonstration of their reduction in intensity in siMK2- and siALOX5-treated cells, respectively (fig. S1A). These effects of Gas6 were not seen in MerTK-silenced macrophages (Fig. 1A), suggesting that Gas6 suppressed the phosphorylation of these kinases through its effect on MerTK. Note that even under control conditions, that is, with cells incubated with conditioned medium from mock-transfected HEK 293 cells, basal p-CaMKII abundance in MERTK siRNA–treated cells was modestly increased compared to that in scrambled siRNA–treated macrophages. This was likely due to a low amount of Gas6 in the control medium, because when cells were incubated in phosphate-buffered saline (PBS) instead of control medium, basal p-CaMKII abundance was not affected by MERTK siRNA (fig. S1B). Protein S, another ligand for TAM receptors that activates MerTK, but not Axl (*31*, *32*), also suppressed the CaMKII–p38–MK2–5-LOX cascade (fig. S1C).

Consistent with our previous data (*14*, *30*), Gas6 reduced the ratio of p–Ser^{271}–5-LOX to total 5-LOX in a MerTK-dependent manner (Fig. 1A). Gas6 also increased the amounts of immunoreactive lipoxin A_4 ($iLXA_4$) and resolvin D1 (iRvD1), as determined by enzyme-linked immunosorbent assay (ELISA) measurements, in scrambled siRNA–treated macrophages but not in siMERTK-treated macrophages (Fig. 1B). Furthermore, as predicted by the decrease in p–Ser^{271}–5-LOX abundance, Gas6 decreased the amount of AA-dependent immunoreactive leukotriene B_4 ($iLTB_4$) in a MerTK-dependent manner (Fig. 1C). These data suggest that Gas6, through MerTK, suppresses a kinase cascade that phosphorylates 5-LOX and concomitantly increases lipoxins at the expense of leukotrienes in human macrophages.

Gas6 inactivates CaMKII by increasing SERCA2 abundance and reducing cytosolic Ca^{2+} concentrations

With respect to how Gas6-MerTK signaling might suppress CaMKII activity, we tested whether the pathway reduced the cytosolic concentration of Ca^{2+}, which would, in turn, reduce CaMKII activity (*33*–*35*). Consistent with this possibility, we found that Gas6 decreased the fluorescence intensity of the Ca^{2+} indicator Fluo3-AM (*36*, *37*) in a time-dependent manner in scrambled siRNA–treated macrophages, but not in siMERTK-treated macrophages (Fig. 2A). These flow cytometric data were confirmed by confocal imaging of the cells (fig. S2A). Furthermore, the cytosolic Ca^{2+} chelator BAPTA-AM mimicked the effect of Gas6 in terms of suppressing the phosphorylation of CaMKII, p38, MK2, and 5-LOX (fig. S2B). Note that the effects of Gas6 and BAPTA-AM were not additive, suggesting that they act through the same mechanism.

We considered the hypothesis that Gas6-MerTK signaling suppressed CaMKII activity by increasing the abundance of SERCA, which transports cytosolic Ca^{2+} into the endoplasmic reticulum (*38*, *39*). Gas6 induced increases in *ATP2A2*, which is the mRNA that encodes SERCA2, and in SERCA2 protein in human macrophages in a MerTK-dependent manner (Fig. 2B). The Gla domain of Gas6, whose gamma carbons are posttranslationally carboxylated, was required for the induction of *ATP2A2* because Gla-deleted Gas6 (Gla-less Gas6) (*31*) was unable to induce an increase in *ATP2A2* (fig. S3A). Moreover, apoptotic cells increased *ATP2A2* expression in macrophages (fig. S3B), as did protein S (fig. S3C), which activates MerTK but not Axl. As further evidence that Axl does not play a substantial role in this pathway, treatment of macrophages with siAXL did not suppress the ability of Gas6 to induce *ATP2A2* (fig. S3D). To further determine whether SERCA plays a role in the Gas6-mediated suppression of CaMKII activity, we tested whether thapsigargin, a SERCA inhibitor (*40*, *41*), blocked Gas6-mediated suppression of the kinase pathway. As predicted, thapsigargin abolished the Gas6-mediated suppression of the phosphorylation of CaMKII, p38, MK2, and 5-LOX (Fig. 2C). Consistent with the proposed sequence of this pathway, we found that *ATP2A2* was increased after 3 hours of Gas6 treatment, whereas p–5-LOX was not decreased until 5 hours after stimulation (fig. S3, E and F). Together, these data support the hypothesis that Gas6-MerTK signaling suppresses CaMKII phosphorylation and the subsequent downstream pathway by inducing *ATP2A2* expression and reducing cytosolic Ca^{2+}.

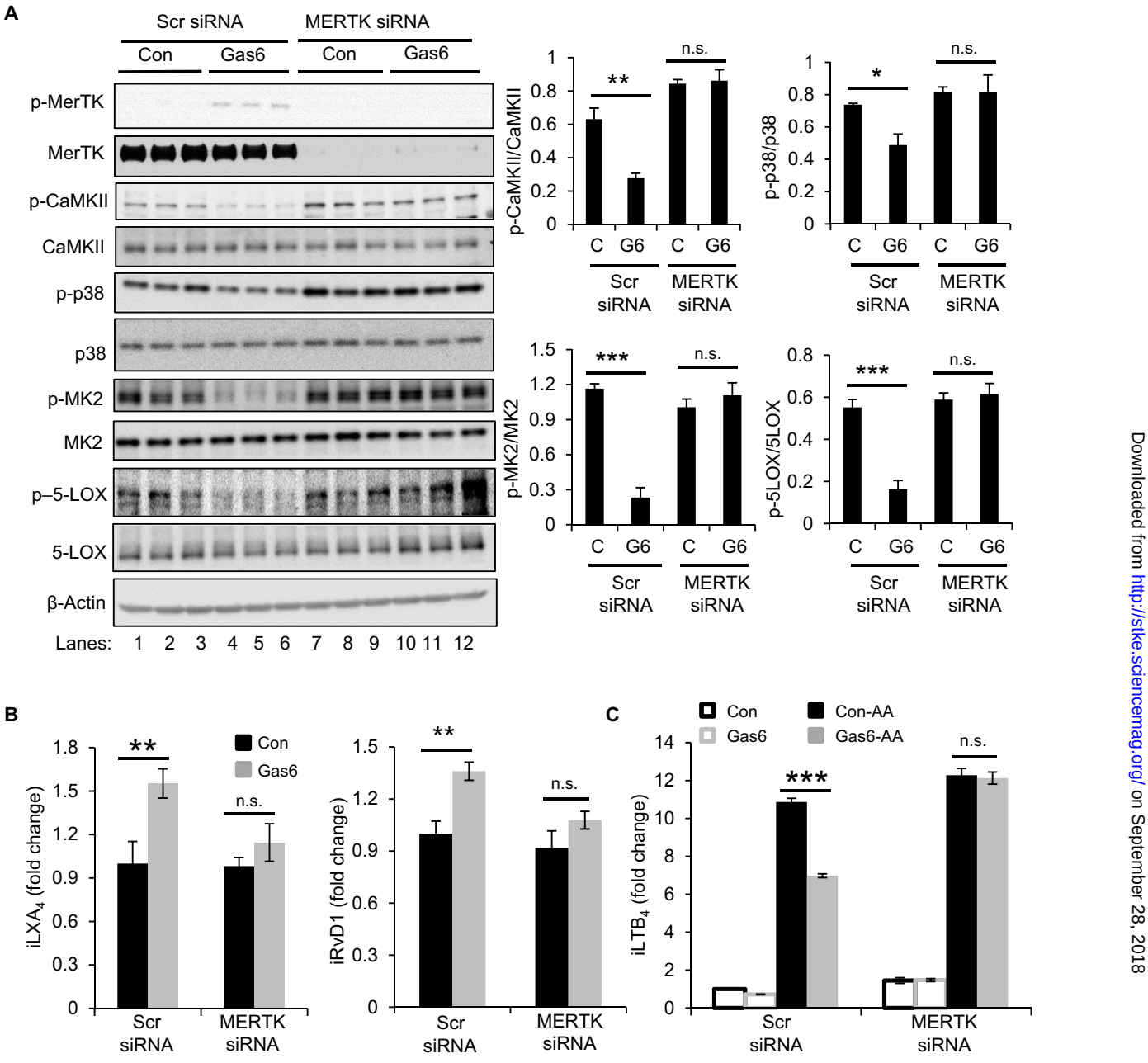

Fig. 1. MerTK is required for Gas6-mediated suppression of the CaMKII–p38–MK2–5-LOX–SPM signaling pathway in human macrophages. (**A** to **C**) Human monocyte–derived macrophages were transfected with either scrambled siRNA or MERTK-specific siRNA. After 72 hours, the cells were incubated for 7 hours with control medium (Con) or 10 nM Gas6-conditioned medium. (A) Left: The macrophages were lysed and analyzed by Western blotting with antibodies specific for phosphorylated (p-) and total MerTK, CaMKII, p38, MK2, and 5-LOX. β-Actin served as the loading control. Blots show samples from three different donors. Right: Bar graphs show the ratio of the amounts of phosphorylated protein to total protein, which was quantified by densitometry with ImageJ software. Data are means ± SEM of three different donors. *$P < 0.05$, **$P < 0.01$, and ***$P < 0.001$ versus control medium by one-way analysis of variance (ANOVA) with post hoc *t* tests for group comparisons; n.s., not significant. (B) Medium from the indicated macrophages was assayed by ELISA to detect $iLXA_4$ and iRvD1. (C) During the last hour of Gas6 treatment, macrophages were incubated with or without 10 μM AA to induce leukotriene production. The amount of $iLTB_4$ in the culture medium was then analyzed by ELISA. Data in (B) and (C) are means ± SEM of three to six donors. **$P < 0.01$ and ***$P < 0.001$ versus control medium by one-way ANOVA with post hoc *t* tests for group comparisons.

Gas6-MerTK signaling induces *ATP2A2* mRNA and SERCA2 protein expression by activating ERK1/2

Previous studies have shown that Gas6-MerTK signaling activates ERK in various cell types, including macrophages (*42*–*45*), and that ERK1/2 induces *ATP2A2* in mouse macrophages (*46*). We therefore investigated whether Gas6-MerTK–induced *ATP2A2* was mediated through ERK1/2 activation. Gas6, protein S, and apoptotic cells increased the abundance of p-ERK in macrophages (Fig. 3A and fig. S4, A and B), and the Gas6-induced increase in p-ERK was substantially reduced in MerTK-silenced macrophages compared to that in

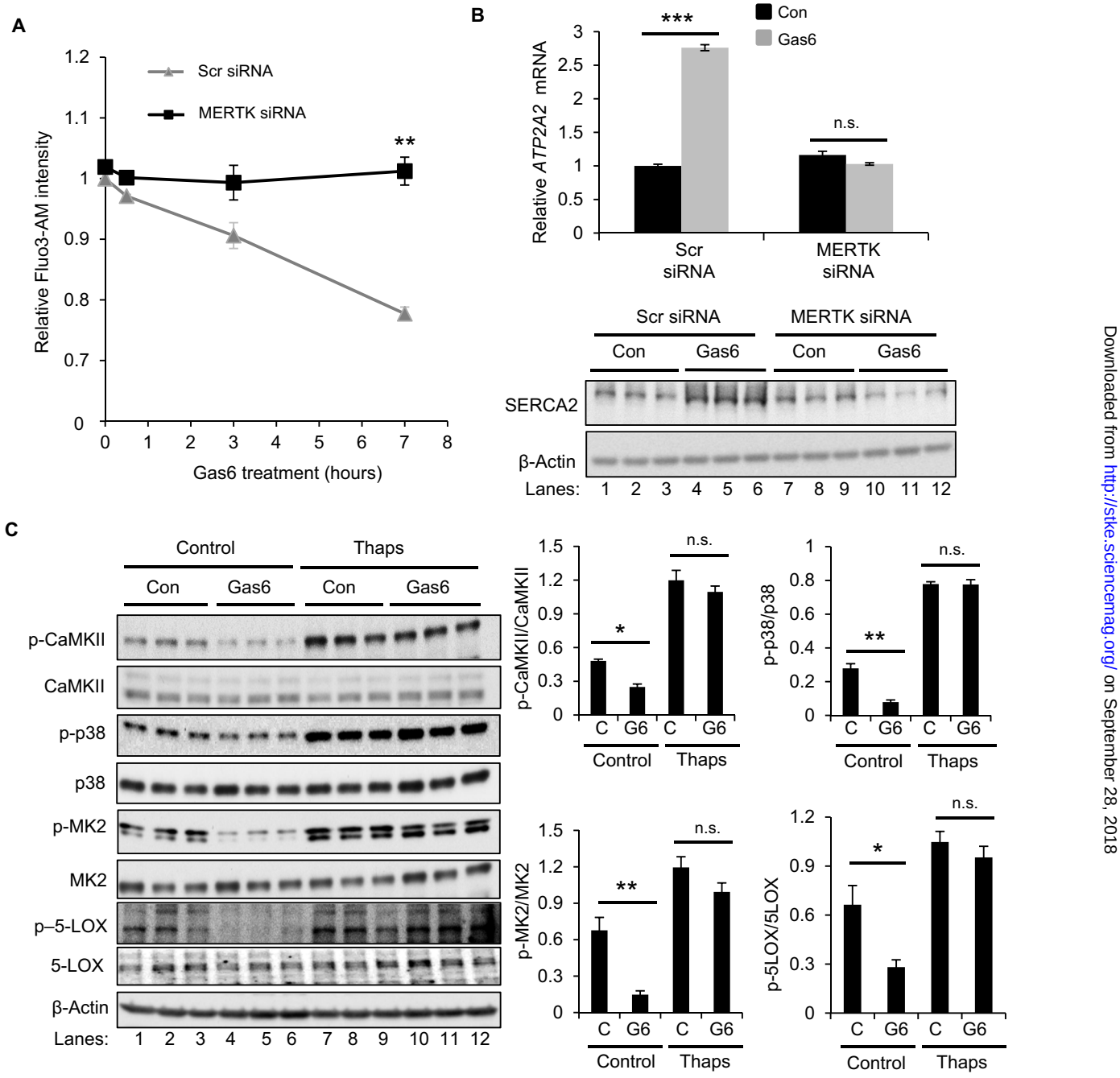

Fig. 2. Gas6 inactivates CaMKII by inducing the expression of *ATP2A2* mRNA and SERCA2 protein and reducing the concentration of cytosolic Ca^{2+}. (**A**) Human macrophages were transfected with scrambled siRNA or MERTK-specific siRNA and were incubated with control or Gas6-conditioned medium for the indicated times. The cells were then loaded with the Ca^{2+} probe Fluo3-AM, and the cytosolic Ca^{2+} concentration was determined by flow cytometry. Data are means ± SEM of three different donors. $^{**}P < 0.01$ versus scrambled siRNA by unpaired *t* test. (**B**) Macrophages transfected with scrambled RNA or MERTK siRNA were incubated with control or Gas6-conditioned medium for 7 hours. The relative abundances of *ATP2A2* mRNA (top) and SERCA2 protein (bottom) were assayed by real-time quantitative polymerase chain reaction (qPCR) and Western blotting analysis, respectively. (**C**) Macrophages were pretreated with 2 μM thapsigargin (Thaps) for 5 min and then incubated with control or Gas6-conditioned medium for 7 hours. Left: Cells were lysed and analyzed by Western blotting with antibodies specific for phosphorylated (p-) and total CaMKII, p38, MK2, and 5-LOX. β-Actin served as the loading control. Blots show samples from three different donors. Right: Bar graphs show the ratios of the amounts of phosphorylated protein to total protein, which were quantified by densitometry with ImageJ software. Data in the bar graphs in (B) and (C) are means ± SEM of three different donors. $^{*}P < 0.05$, $^{**}P < 0.01$, and $^{***}P < 0.001$ versus control medium by one-way ANOVA with post hoc *t* tests for group comparisons.

control cells (Fig. 3A). ERK activation was upstream of *ATP2A2* induction and the subsequent CaMKII–p38–MK2–5-LOX pathway, because both U0126, an inhibitor of the ERK-activating kinases MEK1/2 (*47*, *48*), and ERK-specific siRNA (siERK) suppressed the Gas6-induced expression of *ATP2A2* mRNA and SERCA2 protein, as well as the phosphorylation of components of the CaMKII–p38–MK2–5-LOX cascade (Fig. 3, B and C, and fig. S4, C and D). Consistent with these data, U0126 blocked the ability of Gas6 to increase the abundance of $iLXA_4$ and to decrease that of $iLTB_4$ (Fig. 3D).

MerTK signaling in other scenarios is dependent on tyrosines in its cytoplasmic tail (*49*, *50*). We therefore investigated whether specific tyrosines in MerTK were required for ERK1/2 activation and the suppression of CaMKII phosphorylation. We took advantage of chimeric constructs in which the cytoplasmic tail of wild-type (WT) mouse MerTK, "kinase-deficient" (KD) MerTK, or various tyrosine-to-phenylalanine MerTK mutants are fused with the extracellular domain of CD8 (CDMer) (*49*, *51*). When HEK 293 cells are transfected with plasmid encoding WT CDMer, MerTK signaling is constitutively active, whereas signaling is not seen in cells transfected with plasmid encoding CDMer-KD (*49*, *51*). We found that in WT CDMer–expressing cells, there was a marked increase in ERK1/2 phosphorylation compared with that in mock-transfected or CDMer-KD–expressing cells (Fig. 4A). Furthermore, cells expressing CDMer with mutations at Tyr^{867} and Tyr^{924} showed very little ERK1/2 phosphorylation, whereas ERK1/2 phosphorylation was normal in cells expressing CDMer with a mutation in Tyr^{825} (Fig. 4A). We used flow cytometry to detect cell surface CD8 and found equivalent expression of the WT and mutant receptors (fig. S5).

To test the role of Tyr^{867}, we used retroviruses encoding human WT MerTK or Y872F-mutant MerTK (Tyr^{872} in human MerTK is equivalent to Tyr^{867} in mouse MerTK) to transduce macrophages lacking endogenous MerTK (macrophages from *Mertk*$^{-/-}$ mice). Transduced macrophages expressing WT MerTK recapitulated the Gas6-induced increase in p-ERK1/2 abundance and decrease in p-CaMKII abundance, and, consistent with the above data with CDMer-expressing HEK 293 cells, these effects of Gas6 were abrogated in macrophages expressing Y872F-mutant MerTK (Fig. 4B). These changes in the abundances of p-ERK1/2 and p-CaMKII were verified by flow cytometry (fig. S6A). Flow cytometry also showed that WT and Y872F MerTK were similarly abundant on the cell surface, indicating similar transfection efficiencies of the two constructs, and that Gas6 induced the phosphorylation of WT but not Y872F-MerTK (fig. S6B). These data, when considered together with the data from the experiments using U0126 and siERK, show that the ability of Gas6 to activate the SERCA–CaMKII–5-LOX pathway depends on ERK1/2 activation through a mechanism requiring specific tyrosine residues in the cytoplasmic tail of MerTK.

MEK inhibition delays inflammation resolution in zymosan-induced peritonitis

To determine whether the MEK-ERK pathway was required for resolution of inflammation in vivo, we turned to zymosan-induced peritonitis, a model in which resolution has been shown to be dependent on MerTK (*30*). WT mice were injected intraperitoneally with zymosan in the absence or presence of U0126, and then the number of exudate neutrophils was measured over time to follow the inflammation and resolution stages. The number of neutrophils peaked at 12 hours (T_{max}) and then declined in both groups of mice, but the decline was slower in the U0126-treated mice: the time to a 50% reduction of the peak value (T_{50}) was ~21 hours in vehicle [dimethyl sulfoxide (DMSO)]–treated mice as compared to ~29 hours in the U0126-treated mice, yielding resolution intervals ($R_i = T_{50} - T_{max}$) of 9 and 17 hours, respectively (Fig. 5A). These data are consistent with the notion that MEK1/2 inhibition delays inflammation resolution.

In the next set of experiments, we injected the mice with U0126 during the period when resolving macrophages accumulate in the peritoneum (64 hours after injection with zymosan) (*52*, *53*) and then conducted our assays 8 hours later. We also compared WT and *Mertk*$^{-/-}$ mice in this experiment to determine whether MerTK and MEK-ERK inhibition acted in the same pathway to stimulate resolution. As predicted from the earlier data (Fig. 5A), the number of neutrophils was greater in the U1026-treated WT mice (Fig. 5B), indicating impaired resolution (*14*, *30*). As reported previously (*30*), loss of MerTK also resulted in impaired resolution, and the effects of U0126 and MerTK deletion were not additive (Fig. 5B, second pair of bars). The amount of p-CaMKII in peritoneal macrophages from zymosan-treated WT mice was also increased by U0126 and MerTK deletion in a nonadditive manner (Fig. 5C), and the amount of proresolving $iLXA_4$ in these cells was decreased by both U0126 and MerTK deletion, also in a nonadditive manner (Fig. 5D). These data suggest that the MerTK–ERK–CaMKII-lipoxin pathway functions to resolve inflammation in vivo (fig. S7).

DISCUSSION

The data here reveal a signaling pathway in human macrophages that links MerTK activation with the suppression of CaMKII activity, LXA_4 and RvD1 synthesis, and the resolution of inflammation. A key question is how MerTK becomes activated in vivo to dampen inflammation and promote resolution. Likely candidates include apoptotic cells and Gas6, both of which increase in abundance with inflammation (*54*, *55*). Other MerTK ligands that might be involved include protein S, Tubby, tubby-like protein 1 (Tulp1), and galectin-3 (*56*). However, the relative contribution of different MerTK activators in inflammation and resolution remains unknown and almost certainly varies in different physiologic and pathophysiologic settings. MerTK signaling also suppresses the transcriptional activity of NF-κB in response to lipopolysaccharide (LPS) (*27*, *50*, *57*, *58*), suggesting that MerTK both suppresses inflammation and enhances resolution through separate signaling pathways and effector mechanisms. Furthermore, the NF-κB–suppressing action of MerTK, similar to its proresolution function described here, requires the presence of Tyr^{867} in its cytoplasmic tail (*50*).

A key mediator in the MerTK-induced resolution of inflammation is the suppression of CaMKII activity, which is also the case with RvD1-mediated resolution in macrophages (*14*). In this context, a study from our group showed that in fat-fed *Ldlr*$^{-/-}$ mice, genetic targeting of *Camk2g* in myeloid cells, which encodes the major isoform of myeloid CaMKII, CaMKIIγ, improves efferocytosis, decreases necrosis, and increases fibrous cap thickness in advanced atherosclerotic lesions, suggesting an improved resolution response (*59*). Furthermore, myeloid cell–specific deletion of *Camk2g* led to an increase in cell-surface MerTK through a pathway involving induction of the *Mertk* inducer, liver X receptor α (LXRα) (*59*). These findings are suggestive of a positive feedback cycle in inflammation resolution and efferocytosis in which MerTK activation suppresses CaMKII activity, which then leads to increased MerTK abundance.

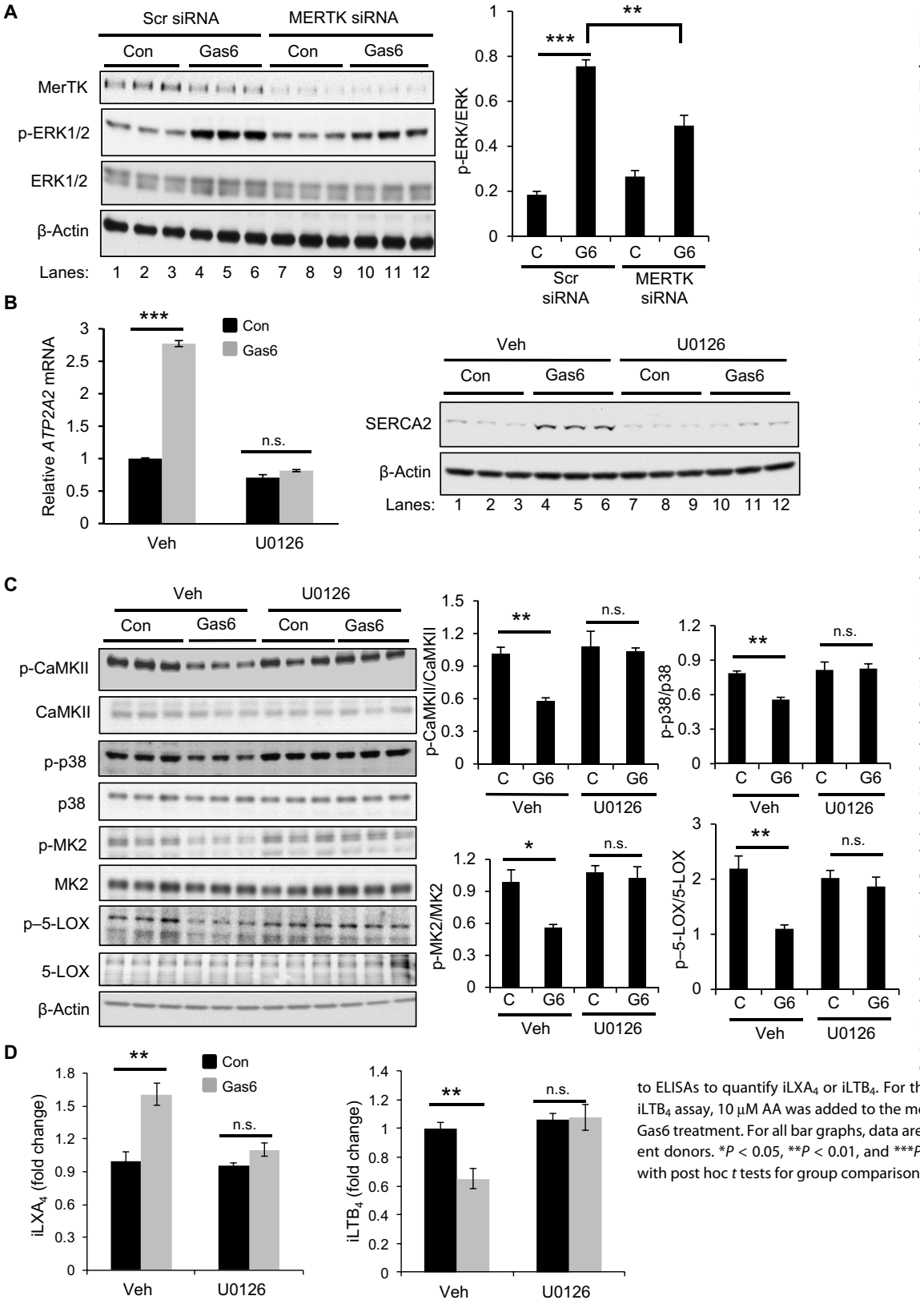

Fig. 3. Gas6-MerTK signaling induces the expression of *ATP2A2* mRNA and SERCA2 protein in human macrophages by activating ERK. (**A**) Human macrophages transfected with scrambled siRNA or MERTK-specific siRNA were incubated with control or Gas6-conditioned medium for 30 min, lysed, and then analyzed by Western blotting with antibodies specific for MerTK, p-ERK1/2, ERK1/2, and β-actin (loading control). Left: Western blots show samples from three different donors. Right: Densitometric analysis of the ratio of the abundances of p-ERK1/2 to total ERK1/2. (**B**) Macrophages were pretreated with vehicle or 10 μM U0126 for 30 min and then incubated with control or Gas6-conditioned medium for 7 hours. The cells were then analyzed by real-time qPCR and Western blotting analysis, respectively, to determine the relative abundances of *ATP2A2* mRNA (left) and SERCA2 protein (right). Western blots show samples from three different donors. (**C**) Macrophages were treated as described in (B) and then were analyzed by Western blotting with antibodies specific for phosphorylated (p-) and total CaMKII, p38, MK2, and 5-LOX. β-Actin served as the loading control. Left: Western blots show samples from three different donors. Right: Bar graphs show the ratios of the indicated phosphorylated protein to total protein, which were quantified by densitometry with ImageJ software. (**D**) Macrophages were treated as described in (B), after which the culture medium was subjected to ELISAs to quantify $iLXA_4$ or $iLTB_4$. For the macrophages used for the $iLTB_4$ assay, 10 μM AA was added to the medium during the last hour of Gas6 treatment. For all bar graphs, data are means ± SEM of three different donors. *$P < 0.05$, **$P < 0.01$, and ***$P < 0.001$ by one-way ANOVA with post hoc *t* tests for group comparisons.

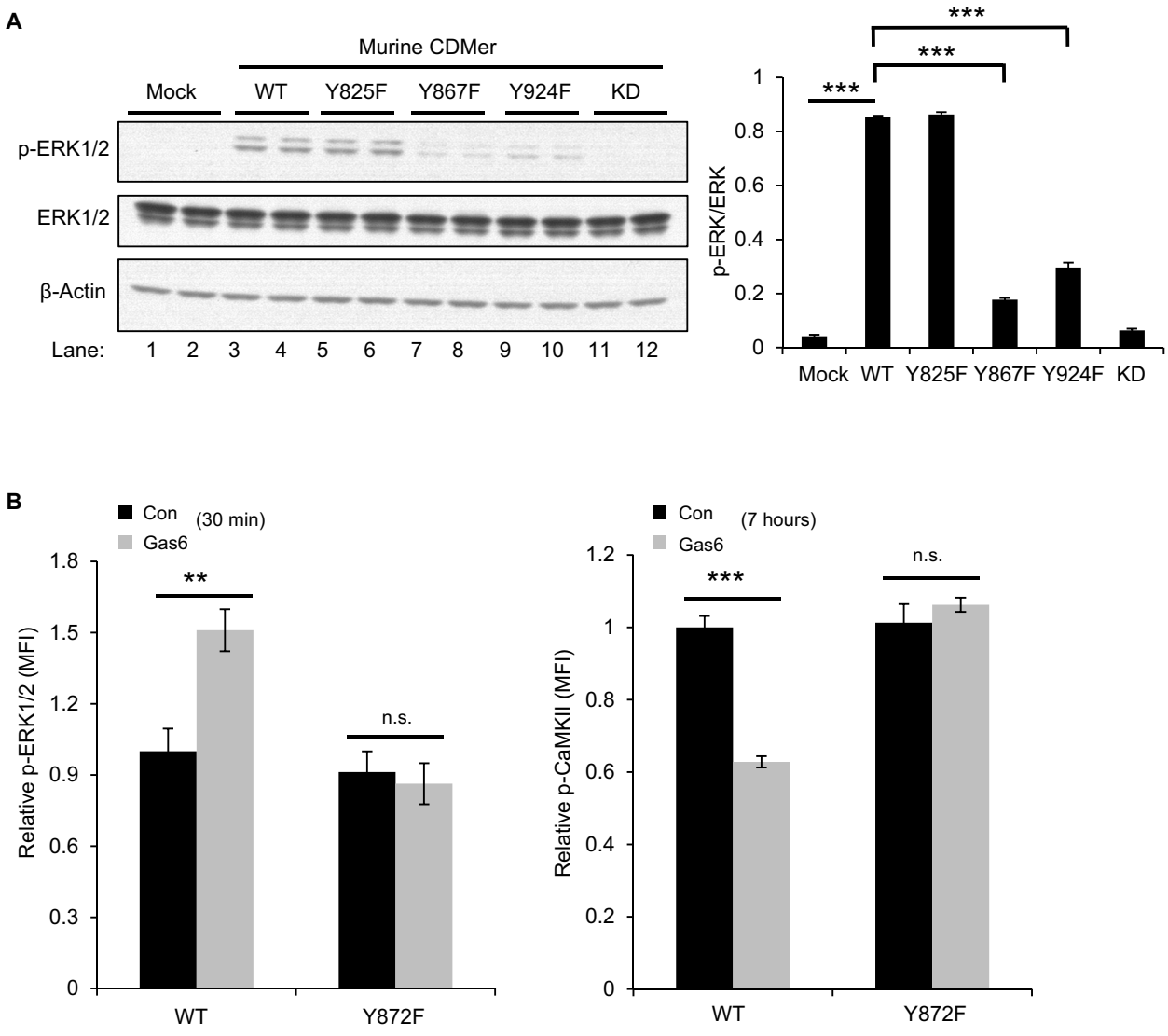

Fig. 4. Specific tyrosine residues in the cytoplasmic tail of MerTK are required for the activation of ERK and CaMKII. (**A**) HEK 293 cells were transfected with various CDMer plasmids encoding WT MerTK, the Y825F, Y867F, and Y924F mutants, and the KD mutant. Forty-eight hours later, the cells subjected to the transfection procedure without plasmids served as control ("Mock"). The cells were lysed and analyzed by Western blotting with antibodies specific for p-ERK1/2, ERK1/2, and β-actin. The bar graph shows the ratios of phosphorylated ERK1/2 to total ERK1/2, which were quantified by densitometry with ImageJ software. Data are means ± SEM of three independent experiments. ***$P < 0.001$ versus WT by one-way ANOVA with post hoc *t* tests for group comparisons. (**B**) Bone marrow–derived macrophages (BMDMs) from *Mertk*$^{-/-}$ mice were transduced with pMSCV–human *MERTK* (WT) or pMSCV–human *MERTK* Y872F. Seventy-two hours later, the cells were then incubated with control or Gas6-conditioned medium for 30 min (left) or 7 hours (right), which was followed by flow cytometric quantification of p-ERK1/2 or p-CaMKII, respectively. Data are means ± SEM of three different mice. **$P < 0.01$ and ***$P < 0.001$ versus control medium by one-way ANOVA with post hoc *t* tests for group comparisons. MFI, mean fluorescence intensity.

The improvements in atherosclerotic plaque endpoints seen in mice with myeloid cell–specific CaMKII deletion were very similar to those seen in *Ldlr*$^{-/-}$ mice with genetically increased MerTK activity, and in that case, we showed directly that the ratio of SPMs to leukotrienes in atherosclerotic lesions was increased (*26*). In another scenario relevant to resolution, mice lacking CaMKII in cardiomyocytes exhibit a blunted inflammatory response after myocardial infarction (*60*). As with genetically increased MerTK activity, deletion of CaMKII may also directly suppress inflammation. For example, the inflammatory response in macrophages treated with LPS and other Toll-like receptor activators in vitro has been associated with CaMKII activation (*61*–*63*).

Activated receptor tyrosine kinases can recruit growth factor receptor–binding protein 2 (Grb2) to their phosphorylated tyrosine residues, leading to the activation of a Ras–Raf–MEK–ERK1/2 cascade (*64*). Tyr^{872} in human MerTK (which is equivalent to Tyr^{867} in murine MerTK) binds to Grb2 and initiates cell survival signaling (*51*, *65*). Consistent with this finding, we found that Tyr^{872} was required for Gas6-induced ERK activation and suppression of CaMKII activity. Note that ERK can trigger both inflammatory and anti-inflammatory responses (*66*–*68*). With regard to our findings, ERK cooperates with SPMs to promote resolution. A previous study showed that, inhibition of ERK by a MEK1 inhibitor abolishes RvE1-mediated phagocytosis of zymosan A by human macrophages (*69*). As another example,

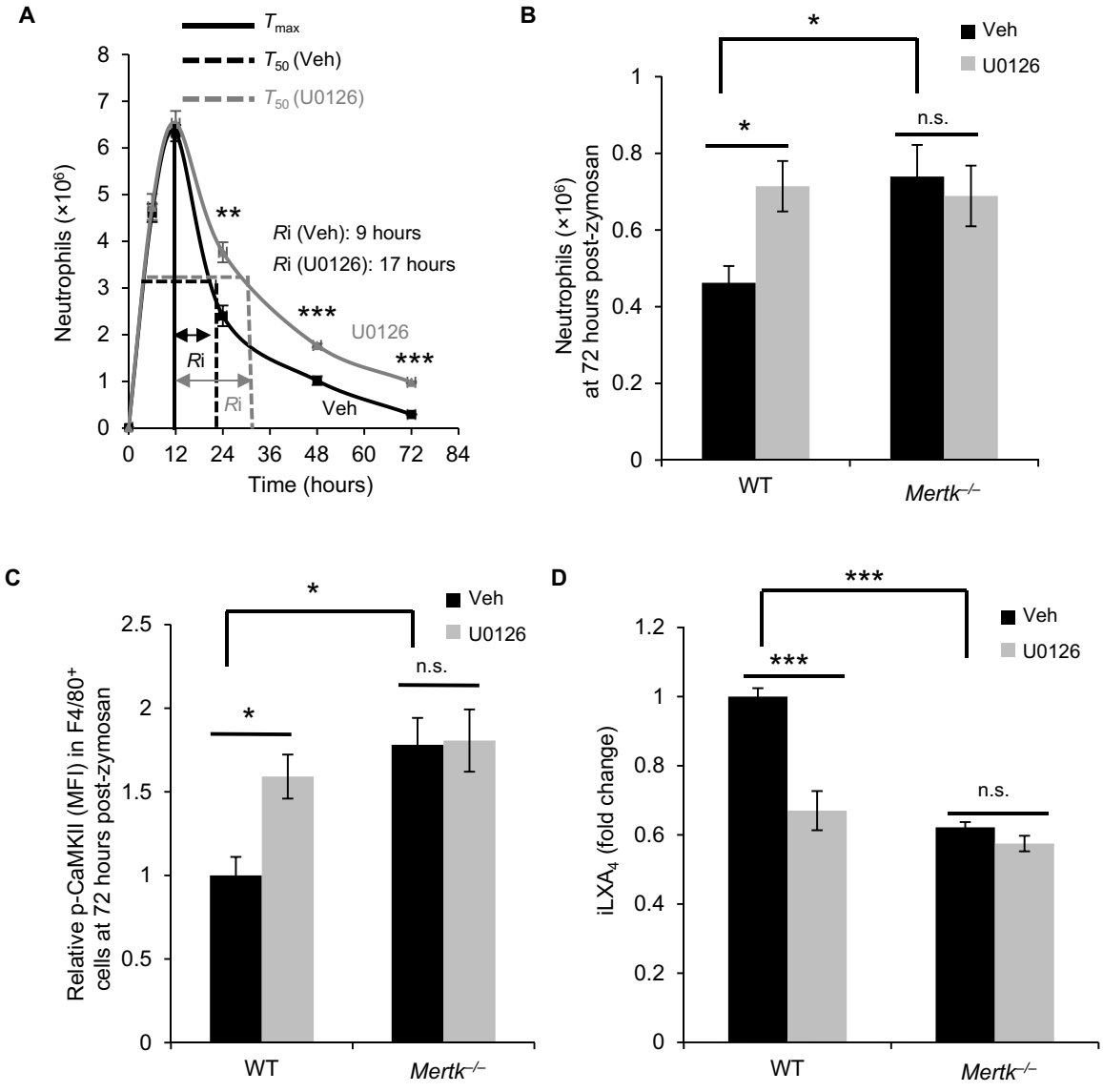

Fig. 5. ERK inhibition suppresses inflammation resolution in zymosan-induced peritonitis in mice. (**A**) WT mice were co-injected intraperitoneally with 0.1 mg of zymosan and either U0126 (25 μg/kg) or an equal volume of DMSO as the vehicle control. Peritoneal exudates were collected by lavage with 3 ml of cold PBS at the indicated times, and leukocytes and exudate fluid were separated by centrifugation at 500*g* for 10 min. Total leukocyte number in the exudate was counted with a hemocytometer, and the percentage of Ly6G$^+$ neutrophils was determined by flow cytometry. Neutrophil number was calculated as total leukocytes × percentage of neutrophils. Resolution intervals (R_i) were calculated as previously described (*30*). Data are means ± SEM of four mice per group. $^{**}P < 0.01$ and $^{***}P < 0.001$ versus vehicle-treated mice by unpaired *t* test. (**B** to **D**) WT or *Mertk*$^{-/-}$ mice were injected intraperitoneally with zymosan, which was followed 64 hours later by intraperitoneal injection with U0126 or DMSO. After an additional 8 hours, peritoneal exudates were collected. (B) Neutrophil number was calculated as described in (A). (C) Peritoneal leukocytes were stained with phycoerythrin (PE)–conjugated anti-F4/80 antibody, which was followed by fixation and permeabilization. Permeabilized cells were stained with anti–p-CaMKII antibody and then an Alexa Fluor 647–conjugated secondary antibody. The MFI of p-CaMKII in the macrophages was quantified by flow cytometry. (D) Exudate iLXA$_4$ was assayed by ELISA. For (B) to (D), data are means ± SEM of four mice per group. $^{*}P < 0.05$ and $^{***}P < 0.001$ versus vehicle-treated WT mice by one-way ANOVA with post hoc *t* tests for group comparisons.

annexin A1, a proresolving mediator, activates ERK and inhibits the interaction of neutrophils with the endothelium (*70*). Furthermore, ERK1/2 signaling is activated in macrophages in which apoptotic cells were recognized by the efferocytosis receptor LDL (low-density lipoprotein) receptor–related protein 1 (LRP1), and ERK activation then facilitates internalization of the apoptotic cells by the macrophages (*71*). Thus, it is possible that LRP1-mediated efferocytosis also activates the resolution pathway described here and that ERK activation in MerTK-activated macrophages contributes to the internalization of apoptotic cells in addition to enhancing resolution. Finally, mouse macrophages that are resistant to the actions of insulin, which occur in the setting of type 2 diabetes, show ERK inhibition-mediated suppression of *ATP2A2* mRNA and SERCA2 protein and depletion of endoplasmic reticulum Ca^{2+}, suggesting that ERK prevents SERCA-mediated Ca^{2+} release into the cytoplasm by inducing in this setting (*46*). These findings, when considered with our findings and those in the aforementioned CaMKII-atherosclerosis study, suggest a possible mechanism linking insulin resistance and type 2 diabetes to accelerated atherosclerotic vascular disease.

In summary, we have elucidated a previously uncharacterized MerTK signaling pathway in macrophages that leads to an enhanced resolution response. In view of the role of impaired resolution in many critical chronic inflammatory diseases, the therapeutic potential of these findings warrants consideration. On the one hand, direct administration of resolving mediators is undergoing extensive preclinical testing for various inflammatory diseases, with early human trials in progress (*72*). However, the possibility of stimulating a natural pathway of resolving mediator synthesis is appealing. The challenges of leveraging the pathway described here for that purpose include identifying specific MerTK activators that do not have non–MerTK-mediated adverse effects (*56*), such as those that have been implicated in oncogenesis (*73*). In-depth study of MerTK signaling pathways in different in vivo settings will be needed to determine whether and how these challenges can be overcome (*74*).

MATERIALS AND METHODS

Preparation of human monocyte–derived macrophages and mouse BMDMs

To generate human macrophages, we isolated monocytes from the buffy coats of de-identified healthy volunteers (New York Blood Center) as previously described (*30*). Briefly, buffy coats were gently layered onto Histopaque solution (Sigma-Aldrich) as 1:1 ratio (v/v) and centrifuged at 1500*g* for 25 min. Leukocytes were removed from the middle layer, washed with RPMI, and then centrifuged at 1500*g* for 5 min. This wash step was repeated once, and then the cell pellet was suspended in RPMI and plated into 12-well plates. After 3 to 4 hours, when monocytes were adherent, the medium was exchanged for RPMI containing 10% (v/v) fetal bovine serum (FBS), 1% penicillin-streptomycin, and recombinant human granulocyte-macrophage colony-stimulating factor (10 ng/ml; PeproTech), and the cells were incubated for 7 to 10 days to allow macrophage differentiation. To generate mouse BMDMs, bone marrow cells were cultured in Dulbecco's modified Eagle's medium (DMEM) containing 10% (v/v) FBS, 1% penicillin-streptomycin, and macrophage colony-stimulating factor, as described previously (*14*, *30*).

siRNA treatment

Human macrophages were incubated in medium containing 50 nM ON-TARGETplus Human MERTK siRNA, MK2 siRNA, ALOX5 siRNA, ERK siRNA, or scrambled siRNA (Dharmacon) and Lipofectamine RNAiMAX (Thermo Fisher Scientific). After 72 hours, the experiments were conducted as indicated in the figure legends.

Treatment of macrophages with Gas6 or protein S

Conditioned medium containing γ-carboxylated Gas6 was harvested from human Gas6-expressing HEK 293-6E cells incubated with vitamin K (2 μg/ml), as described previously (*30*, *32*). The concentration of Gas6 in the medium was 250 nM as determined by comparing the Gas6 signal from a Western blot, quantified by densitometry, with that of a standard curve generated through Western blotting and quantification of multiple concentrations of commercial recombinant human Gas6 (R&D Systems). Macrophages were washed with PBS three times, preincubated for 1 hour in serum-free DMEM, and then incubated in serum-free DMEM with a 1:25 dilution of conditioned medium, equivalent to 10 nM γ-carboxylated Gas6, or an equal volume of conditioned medium from nontransfected HEK 293 cells, which is referred to in the figures as "control" (Con) at the indicated times. Alternatively, macrophages were treated with 100 nM protein S, which was purified from human plasma (Haematologic Technologies).

Western blotting

Cell extracts were resolved on 4 to 20% gradient SDS-polyacrylamide gels and transferred to 0.45-μm nitrocellulose membranes. The membranes were blocked in tris-buffered saline/0.1% Tween 20 (TBST) containing 5% (w/v) nonfat milk at room temperature for 1 hour and then incubated with the primary antibody in TBST containing 5% (w/v) nonfat milk or 5% (w/v) BSA (bovine serum albumin) at 4°C overnight. The membranes were then incubated with the appropriate secondary antibody coupled to horseradish peroxidase (HRP), and proteins were detected with the ECL SuperSignal West Pico Chemiluminescent Substrate kit (Thermo Fisher Scientific). Antibodies used for the Western blotting were as follows: anti–p-CaMKII (Thr^{286}) (Novus); anti-CaMKII (Santa Cruz Biotechnology); anti-SERCA2, anti–p-ERK1/2 (Thr^{202}/Tyr^{204}), anti–p–5-LOX (Ser^{271}), anti–5-LOX, anti–p-MK2 (Thr^{334}), anti-MK2, anti–p-p38 MAPK (Thr^{180}/Tyr^{182}), anti–p38 MAPK, and anti–HRP–β-actin (Cell Signaling Technology); anti–p-MerTK (PMKT-140AP, FabGennix); and anti-MerTK (ab52968, Abcam).

SPM ELISAs

Human macrophages in 12-well plates were incubated for 7 hours at 37°C with vehicle or 10 nM γ-carboxylated Gas6. The cell culture medium was then harvested for analysis by (i) the Neogen LXA_4 ELISA kit, which has the following cross-reactivities according to the manufacturer: 15-epi-LXA_4 (24%), 5(S),6(R)-DiHETE (5%), LXB_4 (1%), and 15-HETE (0.1%); (ii) the Cayman LTB_4 ELISA kit, which has cross-reactivities to 5,6-DiHETE (0.07%), 5(R)-HETE (3.7%), 15(R)-HETE (0.98%), 15(S)-HETE (0.4%), 5(S)-HETE (6.6%), 20-hydroxy LTB_4 (2.7%), 6-*trans*-12-*epi* LTB_4 (0.31%), and 6-*trans* LTB_4 (0.11%); or (iii) the Cayman RvD1 ELISA kit, which has cross-reactivities to 5(S),6(R)-LXA_4 (20%), 17(R)-RvD1 (4.2%), and 10(S),17(S)-DiHDoHE (0.7%). We refer to these lipid mediators as $iLXA_4$, $iLTB_4$, and iRvD1, respectively, where "i" stands for "immunoreactive." The data are reported as fold change in abundance in the experimental group relative to that in the control group, which was set at 1.0. Similar analyses were conducted on peritoneal exudates for the zymosan experiments. In all cases, 50 μl of sample was assayed as per the manufacturer's instructions.

Fluo3-AM loading

Human macrophages were loaded with 1.25 μm of Fluo3-AM (Thermo Fisher Scientific) for 30 min at room temperature in loading buffer containing 150 mM NaCl, 5 mM KCl, 1 mM $MgCl_2$, 1 mM $CaCl_2$, 20 mM Hepes, 10 mM glucose, 1× PowerLoad (Thermo Fisher Scientific) to solubilize the Fluo3-AM dye, and 2.5 mM probenecid (Thermo Fisher Scientific) for dye retention. Fluo3-AM was then removed, and the cells were chased in loading buffer without PowerLoad and probenecid for 30 min at room temperature. Cytosolic Ca^{2+} was monitored by flow cytometry (FACSCanto II) or with a Nikon A1 confocal microscope.

Transfection of HEK 293T cells with plasmids expressing CDMer constructs

Retroviral expression vectors pLXSN expressing a chimeric receptor (CDMer) generated from the extracellular and transmembrane domains of human CD8 (amino acids 1 to 209) and the intracellular

region (amino acids 521 to 994) of WT MerTK, K614M KD MerTK, Y825F MerTK, Y867F MerTK, or Y924F MerTK were generated and used to transfect HEK 293T cells as described previously (*49*, *50*).

Generation of human WT and Y872F *MERTK* pMSCV vectors for transduction into *Mertk*$^{-/-}$ mouse macrophages

Human *MERTK* (NM_006343.2) was cloned into pMSCV-puro retroviral vector (Addgene) at the Xho I and Eco RI restriction sites (Genewiz). Tyr^{872} of human *MERTK* was mutated to phenylalanine using the PCR-based QuikChange mutagenesis system (Stratagene). BOSC23 cells (5×10^6 cells) were transfected with 1 μg of pMSCV-WT Mertk or pMSCV-Y872F *MERTK* together with 1 μg of pCL-Eco (Addgene) and 2 μg of pMD2.G (Addgene) using 16 ml of LipoD293 transfection reagent (SignaGen). Conditioned medium was collected 48 hours after transfection and filtered through 0.45-μm filters. The medium was then used to transduce BMDMs from *Mertk*$^{-/-}$ mice.

Zymosan A–induced peritonitis

Eight- to 10-week-old C57BL/6J mice were injected intraperitoneally with 0.1 mg of zymosan A (Sigma-Aldrich) per mouse. Peritoneal exudates were collected by lavage with 3 ml of cold PBS after 72 hours. Peritoneal leukocytes and exudate fluids were separated by centrifugation at 500*g* for 10 min. Mice were randomly assigned to treatment groups. All procedures were conducted in accordance with the guidelines for animal care of the Columbia University Institutional Animal Care and Use Committee.

Flow cytometric assays

For the zymosan-induced peritonitis experiments, peritoneal exudate cells harvested at the times indicated in the figure legend were washed with fluorescence-activated cell sorting (FACS) staining buffer [PBS containing 3% (v/v) FBS]. The cells were incubated for 5 min at 4°C with Fc Block (BD Biosciences) and then labeled with Pacific Blue–Ly6G (clone 1A8, eBioscience) to detect polymorphonuclear neutrophils. To detect p-CaMKII in exudate macrophages, cells were stained with PE-F4/80 (clone BM8, eBioscience) for 30 min at 4°C to stain macrophages, which was followed by fixation and permeabilization of the cells. Permeabilized cells were then incubated with rabbit anti–p-CaMKII for 1 hour at 4°C and then with Alexa Fluor 647–conjugated goat anti-rabbit secondary antibody for 30 min at 4°C. For the flow cytometric assay of p-ERK and p-CaMKII in WT MerTK–expressing versus Y872F MerTK–expressing *Mertk*$^{-/-}$ macrophages, the cells were first incubated with allophycocyanin (APC)–MerTK (clone #125518, R&D Systems) to label transduced macrophages. After fixation and permeabilization, the cells were incubated with rabbit anti–p-ERK or anti–p-CaMKII antibodies, which was followed by incubation with PE-conjugated anti-rabbit secondary antibody. The cells were suspended in FACS buffer and analyzed for the MFI of p-ERK and p-CaMKII in APC-MerTK^{+} cells gated using a FACSCanto II (BD Biosciences) flow cytometer and FlowJo software.

Apoptotic cell preparation and addition to macrophages

Jurkat cells were exposed to ultraviolet light at 254 nm for 5 min using a lamp from Ultra-Violet Products Ltd. and then incubated in a 37°C incubator with 5% CO_2 for 3 hours to induce apoptosis as previously described (*75*). Apoptotic Jurkat cells (ACs) were added to human macrophages in the presence of FBS-containing medium for the times indicated in the figure legend. ACs were then removed by rinsing five times with cold PBS, and the abundances of *ATP2A2* mRNA or p-ERK and total ERK were assayed as indicated in the figure legends.

Statistical analysis

All results are shown as means ± SEM. Two-tailed *P* values were calculated using Student's *t* test for just two groups. With more than two groups, one-way ANOVA with post hoc *t* tests was used for group comparisons. One-way ANOVA was also used with two factors, for example, genotype and treatment, to allow for interaction. For example, in Fig. 5, U0126 effects could be different between WT and *Mertk*$^{-/-}$.

SUPPLEMENTARY MATERIALS

www.sciencesignaling.org/cgi/content/full/11/549/eaar3721/DC1

Fig. S1. Validation of the MK2 and 5-LOX antibodies with siRNAs; MerTK deletion does not alter CaMKII activity in the absence of Gas6; and protein S can suppress the CaMKII pathway.

Fig. S2. Gas6 reduces cytosolic Ca^{2+} in a MerTK-dependent manner, and BAPTA-AM suppresses CaMKII–p38–MK2–5-LOX signaling.

Fig. S3. Further studies related to MerTK ligands and demonstration that Axl does not mediate Gas6-induced *ATP2A2* expression.

Fig. S4. Protein S and apoptotic cells activate ERK1/2 in macrophages, and ERK1/2 is required for Gas6-mediated suppression of CaMKII–p38–MK2–5-LOX signaling.

Fig. S5. Detection of the cell surface expression of CDMer proteins in transfected HEK 293 cells.

Fig. S6. Tyr^{872} in the cytoplasmic tail of human MerTK is required for the activation of ERK1/2 and CaMKII.

Fig. S7. Summary scheme of MerTK-mediated resolution signaling.

REFERENCES AND NOTES

1. C. N. Serhan, Pro-resolving lipid mediators are leads for resolution physiology. *Nature* **510**, 92–101 (2014).
2. R. Medzhitov, Inflammation 2010: New adventures of an old flame. *Cell* **140**, 771–776 (2010).
3. C. Nathan, A. Ding, Nonresolving inflammation. *Cell* **140**, 871–882 (2010).
4. J. Viola, O. Soehnlein, Atherosclerosis—A matter of unresolved inflammation. *Semin. Immunol.* **27**, 184–193 (2015).
5. H. H. Arnardottir, J. Dalli, L. V. Norling, R. A. Colas, M. Perretti, C. N. Serhan, Resolvin D3 is dysregulated in arthritis and reduces arthritic inflammation. *J. Immunol.* **197**, 2362–2368 (2016).
6. B. D. Levy, C. Bonnans, E. S. Silverman, L. J. Palmer, G. Marigowda, E. Israel; Severe Asthma Research Program, National Heart, Lung, and Blood Institute, Diminished lipoxin biosynthesis in severe asthma. *Am. J. Respir. Crit. Care Med.* **172**, 824–830 (2005).
7. G. Fredman, J. Hellmann, J. D. Proto, G. Kuriakose, R. A. Colas, B. Dorweiler, E. S. Connolly, R. Solomon, D. M. Jones, E. J. Heyer, M. Spite, I. Tabas, An imbalance between specialized pro-resolving lipid mediators and pro-inflammatory leukotrienes promotes instability of atherosclerotic plaques. *Nat. Commun.* **7**, 12859 (2016).
8. C. N. Serhan, C. B. Clish, J. Brannon, S. P. Colgan, N. Chiang, K. Gronert, Novel functional sets of lipid-derived mediators with antiinflammatory actions generated from omega-3 fatty acids via cyclooxygenase 2-nonsteroidal antiinflammatory drugs and transcellular processing. *J. Exp. Med.* **192**, 1197–1204 (2000).
9. C. N. Serhan, S. Hong, K. Gronert, S. P. Colgan, P. R. Devchand, G. Mirick, R. L. Moussignac, Resolvins: A family of bioactive products of omega-3 fatty acid transformation circuits initiated by aspirin treatment that counter proinflammation signals. *J. Exp. Med.* **196**, 1025–1037 (2002).
10. C. D. Buckley, D. W. Gilroy, C. N. Serhan, Proresolving lipid mediators and mechanisms in the resolution of acute inflammation. *Immunity* **40**, 315–327 (2014).
11. S. C. Dyall, Long-chain omega-3 fatty acids and the brain: A review of the independent and shared effects of EPA, DPA and DHA. *Front Aging Neurosci.* **7**, 52 (2015).
12. T. G. Brock, E. Maydanski, R. W. McNish, M. Peters-Golden, Co-localization of leukotriene a4 hydrolase with 5-lipoxygenase in nuclei of alveolar macrophages and rat basophilic leukemia cells but not neutrophils. *J. Biol. Chem.* **276**, 35071–35077 (2001).
13. M. Luo, S. M. Jones, M. Peters-Golden, T. G. Brock, Nuclear localization of 5-lipoxygenase as a determinant of leukotriene B4 synthetic capacity. *Proc. Natl. Acad. Sci. U.S.A.* **100**, 12165–12170 (2003).
14. G. Fredman, L. Ozcan, S. Spolitu, J. Hellmann, M. Spite, J. Backs, I. Tabas, Resolvin D1 limits 5-lipoxygenase nuclear localization and leukotriene B4 synthesis by inhibiting a calcium-activated kinase pathway. *Proc. Natl. Acad. Sci. U.S.A.* **111**, 14530–14535 (2014).

15. U. P. Kelavkar, W. Glasgow, S. J. Olson, B. A. Foster, S. B. Shappell, Overexpression of 12/15-lipoxygenase, an ortholog of human 15-lipoxygenase-1, in the prostate tumors of TRAMP mice. *Neoplasia* **6**, 821–830 (2004).
16. X. S. Chen, U. Kurre, N. A. Jenkins, N. G. Copeland, C. D. Funk, cDNA cloning, expression, mutagenesis of C-terminal isoleucine, genomic structure, and chromosomal localizations of murine 12-lipoxygenases. *J. Biol. Chem.* **269**, 13979–13987 (1994).
17. H. Kühn, D. Heydeck, R. Brinckman, F. Trebus, Regulation of cellular 15-lipoxygenase activity on pretranslational, translational, and posttranslational levels. *Lipids* **34**, S273–S279 (1999).
18. O. Werz, D. Szellas, D. Steinhilber, O. Rådmark, Arachidonic acid promotes phosphorylation of 5-lipoxygenase at Ser-271 by MAPK-activated protein kinase 2 (MK2). *J. Biol. Chem.* **277**, 14793–14800 (2002).
19. A. Nguyen, P. Chen, H. Cai, Role of CaMKII in hydrogen peroxide activation of ERK1/2, p38 MAPK, HSP27 and actin reorganization in endothelial cells. *FEBS Lett.* **572**, 307–313 (2004).
20. L. Ozcan, J. C. de Souza, A. A. Harari, J. Backs, E. N. Olson, I. Tabas, Activation of calcium/calmodulin-dependent protein kinase II in obesity mediates suppression of hepatic insulin signaling. *Cell Metab.* **18**, 803–815 (2013).
21. G. Lemke, T. Burstyn-Cohen, TAM receptors and the clearance of apoptotic cells. *Ann. N. Y. Acad. Sci.* **1209**, 23–29 (2010).
22. G. Lemke, Biology of the TAM receptors. *Cold Spring Harb. Perspect. Biol.* **5**, a009076 (2013).
23. P. L. Cohen, R. Caricchio, V. Abraham, T. D. Camenisch, J. C. Jennette, R. A. Roubey, H. S. Earp, G. Matsushima, E. A. Reap, Delayed apoptotic cell clearance and lupus-like autoimmunity in mice lacking the c-mer membrane tyrosine kinase. *J. Exp. Med.* **196**, 135–140 (2002).
24. E. Thorp, D. Cui, D. M. Schrijvers, G. Kuriakose, I. Tabas, Mertk receptor mutation reduces efferocytosis efficiency and promotes apoptotic cell accumulation and plaque necrosis in atherosclerotic lesions of apoe$^{-/-}$ mice. *Arterioscler. Thromb. Vasc. Biol.* **28**, 1421–1428 (2008).
25. H. Ait-Oufella, V. Pouresmail, T. Simon, O. Blanc-Brude, K. Kinugawa, R. Merval, G. Offenstadt, G. Lesèche, P. L. Cohen, A. Tedgui, Z. Mallat, Defective mer receptor tyrosine kinase signaling in bone marrow cells promotes apoptotic cell accumulation and accelerates atherosclerosis. *Arterioscler. Thromb. Vasc. Biol.* **28**, 1429–1431 (2008).
26. B. Cai, E. B. Thorp, A. C. Doran, B. E. Sansbury, M. J. Daemen, B. Dorweiler, M. Spite, G. Fredman, I. Tabas, MerTK receptor cleavage promotes plaque necrosis and defective resolution in atherosclerosis. *J. Clin. Invest.* **127**, 564–568 (2017).
27. Y. J. Lee, J. Y. Han, J. Byun, H. J. Park, E. M. Park, Y. H. Chong, M. S. Cho, J. L. Kang, Inhibiting Mer receptor tyrosine kinase suppresses STAT1, SOCS1/3, and NF-κB activation and enhances inflammatory responses in lipopolysaccharide-induced acute lung injury. *J. Leukoc. Biol.* **91**, 921–932 (2012).
28. J. Y. Choi, H. J. Park, Y. J. Lee, J. Byun, Y. S. Youn, J. H. Choi, S. Y. Woo, J. L. Kang, Upregulation of Mer receptor tyrosine kinase signaling attenuated lipopolysaccharide-induced lung inflammation. *J. Pharmacol. Exp. Ther.* **344**, 447–458 (2013).
29. J. Y. Choi, J. Y. Seo, Y. S. Yoon, Y. J. Lee, H. S. Kim, J. L. Kang, Mer signaling increases the abundance of the transcription factor LXR to promote the resolution of acute sterile inflammation. *Sci. Sig.* **8**, ra21 (2015).
30. B. Cai, E. B. Thorp, A. C. Doran, M. Subramanian, B. E. Sansbury, C. S. Lin, M. Spite, G. Fredman, I. Tabas, MerTK cleavage limits proresolving mediator biosynthesis and exacerbates tissue inflammation. *Proc. Natl. Acad. Sci. U.S.A.* **113**, 6526–6531 (2016).
31. E. D. Lew, J. Oh, P. G. Burrola, I. Lax, A. Zagórska, P. G. Través, J. Schlessinger, G. Lemke, Differential TAM receptor-ligand-phospholipid interactions delimit differential TAM bioactivities. *eLife* **3**, 10.7554/eLife.03385 (2014).
32. W. I. Tsou, K. Q. Nguyen, D. A. Calarese, S. J. Garforth, A. L. Antes, S. V. Smirnov, S. C. Almo, R. B. Birge, S. V. Kotenko, Receptor tyrosine kinases, TYRO3, AXL, and MER, demonstrate distinct patterns and complex regulation of ligand-induced activation. *J. Biol. Chem.* **289**, 25750–25763 (2014).
33. L. F. Couchonnal, M. E. Anderson, The role of calmodulin kinase II in myocardial physiology and disease. *Physiology (Bethesda)* **23**, 151–159 (2008).
34. H. A. Singer, Ca^{2+}/calmodulin-dependent protein kinase II function in vascular remodelling. *J. Physiol.* **590**, 1349–1356 (2012).
35. L. Ozcan, C. C. Wong, G. Li, T. Xu, U. Pajvani, S. K. Park, A. Wronska, B. X. Chen, A. R. Marks, A. Fukamizu, J. Backs, H. A. Singer, J. R. Yates III, D. Accili, I. Tabas, Calcium signaling through CaMKII regulates hepatic glucose production in fasting and obesity. *Cell Metab.* **15**, 739–751 (2012).
36. E. J. Novak, P. S. Rabinovitch, Improved sensitivity in flow cytometric intracellular ionized calcium measurement using fluo-3/Fura Red fluorescence ratios. *Cytometry* **17**, 135–141 (1994).
37. P. Sundaramoorthy, J. J. Sim, Y. S. Jang, S. K. Mishra, K. Y. Jeong, P. Mander, O. B. Chul, W. S. Shim, S. H. Oh, K. Y. Nam, H. M. Kim, Modulation of intracellular calcium levels by calcium lactate affects colon cancer cell motility through calcium-dependent calpain. *PLOS ONE* **10**, e0116984 (2015).
38. F. N. Reddish, C. L. Miller, R. Gorkhali, J. J. Yang, Calcium dynamics mediated by the endoplasmic/sarcoplasmic reticulum and related diseases. *Int. J. Mol. Sci.* **18**, E1024 (2017).
39. D. E. Clapham, Calcium signaling. *Cell* **131**, 1047–1058 (2007).
40. J. Lytton, M. Westlin, M. R. Hanley, Thapsigargin inhibits the sarcoplasmic or endoplasmic reticulum Ca-ATPase family of calcium pumps. *J. Biol. Chem.* **266**, 17067–17071 (1991).
41. J. M. Timmins, L. Ozcan, T. A. Seimon, G. Li, C. Malagelada, J. Backs, T. Backs, R. Bassel-Duby, E. N. Olson, M. E. Anderson, I. Tabas, Calcium/calmodulin-dependent protein kinase II links ER stress with Fas and mitochondrial apoptosis pathways. *J. Clin. Invest.* **119**, 2925–2941 (2009).
42. L. N. Brandao, A. Winges, S. Christoph, S. Sather, J. Migdall-Wilson, J. Schlegel, A. McGranahan, D. Gao, X. Liang, D. Deryckere, D. K. Graham, Inhibition of MerTK increases chemosensitivity and decreases oncogenic potential in T-cell acute lymphoblastic leukemia. *Blood Cancer J* **3**, e101 (2013).
43. C. T. Cummings, D. Deryckere, H. S. Earp, D. K. Graham, Molecular pathways: MERTK signaling in cancer. *Clin. Cancer Res.* **19**, 5275–5280 (2013).
44. J. Schlegel, M. J. Sambade, S. Sather, S. J. Moschos, A. C. Tan, A. Winges, D. DeRyckere, C. C. Carson, D. G. Trembath, J. J. Tentler, S. G. Eckhardt, P. F. Kuan, R. L. Hamilton, L. M. Duncan, C. R. Miller, N. Nikolaishvili-Feinberg, B. R. Midkiff, J. Liu, W. Zhang, C. Yang, X. Wang, S. V. Frye, H. S. Earp, J. M. Shields, D. K. Graham, MERTK receptor tyrosine kinase is a therapeutic target in melanoma. *J. Clin. Invest.* **123**, 2257–2267 (2013).
45. A. Anwar, A. K. Keating, D. Joung, S. Sather, G. K. Kim, K. K. Sawczyn, L. Brandão, P. M. Henson, D. K. Graham, Mer tyrosine kinase (MerTK) promotes macrophage survival following exposure to oxidative stress. *J. Leukoc. Biol.* **86**, 73–79 (2009).
46. C. P. Liang, S. Han, G. Li, I. Tabas, A. R. Tall, Impaired MEK signaling and SERCA expression promote ER stress and apoptosis in insulin-resistant macrophages and are reversed by exenatide treatment. *Diabetes* **61**, 2609–2620 (2012).
47. F. Marampon, G. Bossi, C. Ciccarelli, A. Di Rocco, A. Sacchi, R. G. Pestell, B. M. Zani, MEK/ERK inhibitor U0126 affects in vitro and in vivo growth of embryonal rhabdomyosarcoma. *Mol. Cancer Ther.* **8**, 543–551 (2009).
48. F. Marampon, G. L. Gravina, A. Di Rocco, P. Bonfili, M. Di Staso, C. Fardella, L. Polidoro, C. Ciccarelli, C. Festuccia, V. M. Popov, R. G. Pestell, V. Tombolini, B. M. Zani, MEK/ERK inhibitor U0126 increases the radiosensitivity of rhabdomyosarcoma cells in vitro and in vivo by downregulating growth and DNA repair signals. *Mol. Cancer Ther.* **10**, 159–168 (2011).
49. Y. Wu, S. Singh, M.-M. Georgescu, R. B. Birge, A role for Mer tyrosine kinase in αvβ5 integrin-mediated phagocytosis of apoptotic cells. *J. Cell Sci.* **118**, 539–553 (2005).
50. N. Tibrewal, Y. Wu, V. D'Mello, R. Akakura, T. C. George, B. Varnum, R. B. Birge, Autophosphorylation docking site Tyr-867 in Mer receptor tyrosine kinase allows for dissociation of multiple signaling pathways for phagocytosis of apoptotic cells and down-modulation of lipopolysaccharide-inducible NF-κB transcriptional activation. *J. Biol. Chem.* **283**, 3618–3627 (2008).
51. M. M. Georgescu, K. H. Kirsch, T. Shishido, C. Zong, H. Hanafusa, Biological effects of c-Mer receptor tyrosine kinase in hematopoietic cells depend on the Grb2 binding site in the receptor and activation of NF-κB. *Mol. Cell. Biol.* **19**, 1171–1181 (1999).
52. J. Newson, M. Stables, E. Karra, F. Arce-Vargas, S. Quezada, M. Motwani, M. Mack, S. Yona, T. Audzevich, D. W. Gilroy, Resolution of acute inflammation bridges the gap between innate and adaptive immunity. *Blood* **124**, 1748–1764 (2014).
53. J. Bystrom, I. Evans, J. Newson, M. Stables, I. Toor, N. van Rooijen, M. Crawford, P. Colville-Nash, S. Farrow, D. W. Gilroy, Resolution-phase macrophages possess a unique inflammatory phenotype that is controlled by cAMP. *Blood* **112**, 4117–4127 (2008).
54. J. Savill, Apoptosis in resolution of inflammation. *J. Leukoc. Biol.* **61**, 375–380 (1997).
55. D. Borgel, S. Clauser, C. Bornstain, I. Bièche, A. Bissery, V. Remones, J. Y. Fagon, M. Aiach, J. L. Diehl, Elevated growth-arrest-specific protein 6 plasma levels in patients with severe sepsis. *Crit. Care Med.* **34**, 219–222 (2006).
56. J. H. van der Meer, T. van der Poll, C. van 't Veer, TAM receptors, Gas6, and protein S: Roles in inflammation and hemostasis. *Blood* **123**, 2460–2469 (2014).
57. T. D. Camenisch, B. H. Koller, H. S. Earp, G. K. Matsushima, A novel receptor tyrosine kinase, Mer, inhibits TNF-α production and lipopolysaccharide-induced endotoxic shock. *J. Immunol.* **162**, 3498–3503 (1999).
58. P. Sen, M. A. Wallet, Z. Yi, Y. Huang, M. Henderson, C. E. Mathews, H. S. Earp, G. Matsushima, A. S. Baldwin Jr., R. M. Tisch, Apoptotic cells induce Mer tyrosine kinase-dependent blockade of NF-κB activation in dendritic cells. *Blood* **109**, 653–660 (2007).
59. A. C. Doran, L. Ozcan, B. Cai, Z. Zheng, G. Fredman, C. C. Rymond, B. Dorweiler, J. C. Sluimer, J. Hsieh, G. Kuriakose, A. R. Tall, I. Tabas, CAMKIIγ suppresses an efferocytosis pathway in macrophages and promotes atherosclerotic plaque necrosis. *J. Clin. Invest.* **127**, 4075–4089 (2017).

60. M. Weinreuter, M. M. Kreusser, J. Beckendorf, F. C. Schreiter, F. Leuschner, L. H. Lehmann, K. P. Hofmann, J. S. Rostosky, N. Diemert, C. Xu, H. C. Volz, A. Jungmann, A. Nickel, C. Sticht, N. Gretz, C. Maack, M. D. Schneider, H. J. Gröne, O. J. Muller, H. A. Katus, J. Backs, CaM kinase II mediates maladaptive post-infarct remodeling and pro-inflammatory chemoattractant signaling but not acute myocardial ischemia/reperfusion injury. *EMBO Mol. Med.* **6**, 1231–1245 (2014).
61. C. Pereira, D. J. Schaer, E. B. Bachli, M. O. Kurrer, G. Schoedon, Wnt5A/CaMKII signaling contributes to the inflammatory response of macrophages and is a target for the antiinflammatory action of activated protein C and interleukin-10. *Arterioscler. Thromb. Vasc. Biol.* **28**, 504–510 (2008).
62. X. Liu, M. Yao, N. Li, C. Wang, Y. Zheng, X. Cao, CaMKII promotes TLR-triggered proinflammatory cytokine and type I interferon production by directly binding and activating TAK1 and IRF3 in macrophages. *Blood* **112**, 4961–4970 (2008).
63. X. Zhou, J. Li, W. Yang, Calcium/calmodulin-dependent protein kinase II regulates cyclooxygenase-2 expression and prostaglandin E2 production by activating cAMP-response element-binding protein in rat peritoneal macrophages. *Immunology* **143**, 287–299 (2014).
64. M. M. McKay, D. K. Morrison, Integrating signals from RTKs to ERK/MAPK. *Oncogene* **26**, 3113–3121 (2007).
65. R. M. Linger, A. K. Keating, H. S. Earp, D. K. Graham, TAM receptor tyrosine kinases: Biologic functions, signaling, and potential therapeutic targeting in human cancer. *Adv. Cancer Res.* **100**, 35–83 (2008).
66. Y. S. Maeng, J. K. Min, J. H. Kim, A. Yamagishi, N. Mochizuki, J. Y. Kwon, Y. W. Park, Y. M. Kim, Y. G. Kwon, ERK is an anti-inflammatory signal that suppresses expression of NF-κB-dependent inflammatory genes by inhibiting IKK activity in endothelial cells. *Cell. Signal.* **18**, 994–1005 (2006).
67. V. A. Vo, J. W. Lee, J. E. Chang, J. Y. Kim, N. H. Kim, H. J. Lee, S. S. Kim, W. Chun, Y. S. Kwon, Avicularin inhibits lipopolysaccharide-induced inflammatory response by suppressing ERK phosphorylation in RAW 264.7 macrophages. *Biomol. Ther. (Seoul)* **20**, 532–537 (2012).
68. E. T. Richardson, S. Shukla, D. R. Sweet, P. A. Wearsch, P. N. Tsichlis, W. H. Boom, C. V. Harding, Toll-like receptor 2-dependent extracellular signal-regulated kinase signaling in mycobacterium tuberculosis-infected macrophages drives anti-inflammatory responses and inhibits Th1 polarization of responding T cells. *Infect. Immun.* **83**, 2242–2254 (2015).
69. T. Ohira, M. Arita, K. Omori, A. Recchiuti, T. E. Van Dyke, C. N. Serhan, Resolvin E1 receptor activation signals phosphorylation and phagocytosis. *J. Biol. Chem.* **285**, 3451–3461 (2010).
70. R. P. Hayhoe, A. M. Kamal, E. Solito, R. J. Flower, D. Cooper, M. Perretti, Annexin 1 and its bioactive peptide inhibit neutrophil-endothelium interactions under flow: Indication of distinct receptor involvement. *Blood* **107**, 2123–2130 (2006).
71. A. W. Jehle, S. J. Gardai, S. Li, P. Linsel-Nitschke, K. Morimoto, W. J. Janssen, R. W. Vandivier, N. Wang, S. Greenberg, B. M. Dale, C. Qin, P. M. Henson, A. R. Tall, ATP-binding cassette transporter A7 enhances phagocytosis of apoptotic cells and associated ERK signaling in macrophages. *J. Cell Biol.* **174**, 547–556 (2006).
72. C. N. Serhan, Treating inflammation and infection in the 21st century: New hints from decoding resolution mediators and mechanisms. *FASEB J.* **31**, 1273–1288 (2017).
73. V. Davra, S. G. Kimani, D. Calianese, R. B. Birge, Ligand activation of TAM family receptors-implications for tumor biology and therapeutic response. *Cancers (Basel)* **8**, E107 (2016).
74. I. Dransfield, S. Farnworth, Axl and Mer receptor tyrosine kinases: Distinct and nonoverlapping roles in inflammation and cancer? *Adv. Exp. Med. Biol.* **930**, 113–132 (2016).
75. Y. Wang, M. Subramanian, A. Yurdagul Jr., V. C. Barbosa-Lorenzi, B. Cai, J. de Juan-Sanz, T. A. Ryan, M. Nomura, F. R. Maxfield, I. Tabas, Mitochondrial fission promotes the continued clearance of apoptotic cells by macrophages. *Cell* **171**, 331–345.e22 (2017).

Funding: This work was supported, in part, by an American Heart Association Postdoctoral Fellowship grant (to B.C.); NIH grant 1K99DK115778 (to B.C.); NIH grant CA165077 and a grant from the New Jersey Health Foundation (to R.B.B.); and NIH grants HL132412, HL075662, and HL127464 (to I.T.). The fluorescence microscopy experiments used the Confocal and Specialized Microscopy Core at Columbia University's Irving Cancer Research Center, and the flow cytometry analyses used the Columbia Center for Translational Immunology/Diabetes and Endocrinology Research Center Flow Core facility, funded, in part, by NIH/National Institute of Diabetes and Digestive and Kidney Diseases Center Grant 5P30DK063608. **Author contributions:** B.C. and I.T. initiated the study. R.B.B. provided critical input in the project design. B.C., C.K., and A.C.D. conducted the experiments. All authors contributed to the data analysis, and R.R. was the statistical consultant for the study. B.C. and I.T. wrote the initial manuscript draft, which was then reviewed and edited by the rest of the authors. **Competing interests:** The authors declare that they have no competing interests. **Data and materials availability:** All data needed to evaluate the conclusions of this study are available in the paper or the Supplementary Materials.

Submitted 31 October 2017
Accepted 8 September 2018
Published 25 September 2018
10.1126/scisignal.aar3721

Citation: B. Cai, C. Kasikara, A. C. Doran, R. Ramakrishnan, R. B. Birge, I. Tabas, MerTK signaling in macrophages promotes the synthesis of inflammation resolution mediators by suppressing CaMKII activity. *Sci. Signal.* **11**, eaar3721 (2018).

Science Signaling

MerTK signaling in macrophages promotes the synthesis of inflammation resolution mediators by suppressing CaMKII activity

Bishuang Cai, Canan Kasikara, Amanda C. Doran, Rajasekhar Ramakrishnan, Raymond B. Birge and Ira Tabas

Sci. Signal. **11** (549), eaar3721.
DOI: 10.1126/scisignal.aar3721

Promoting resolution

The active and coordinated process of inflammation resolution is critical for tissue homeostasis, and defective resolution is associated with chronic inflammatory diseases. Specialized proresolving mediators (SPMs) are fatty acid derivatives that counteract the effects of proinflammatory factors, triggering resolution and tissue repair. SPM biosynthesis depends on the cytosolic localization of the nonphosphorylated form of the lipoxygenase 5-LOX, whereas the nuclear translocation of phosphorylated 5-LOX results in inflammatory leukotriene production. Cai *et al*. showed that signaling by the efferocytosis receptor MerTK in macrophages activated an ERK-dependent pathway that inhibited the phosphorylation of 5-LOX, thus promoting SPM production. Inhibition of ERK activation in a mouse model of peritonitis delayed resolution, suggesting that the MerTK-ERK pathway might be therapeutically manipulated to promote inflammation resolution.